Available online at www.sciencedirect.com
SCIENCE DIRECT
Journal of Power Sources 154 (2006) 223–231
JOURNAL OF POWER SOURCES
www.elsevier.com/locate/jpowsour

Catalytic autothermal reforming of diesel fuel for hydrogen generation in fuel cells
II. Catalyst poisoning and characterization studies

Praveen K. Cheekatamarla *, Alan M. Lane

Department of Chemical Engineering, Box 870203, The University of Alabama, Tuscaloosa, AL 35487, USA

Received 24 March 2005; received in revised form 21 April 2005; accepted 21 April 2005
Available online 13 June 2005

Abstract

Hydrogen for use in fuel cells is produced in a fuel processor by the catalytic reforming of hydrocarbons. Experimental results from synthetic diesel and JP8 autothermal reforming activity tests performed over a commercial Pt/ceria catalyst was presented in part I of this paper. A reversible–irreversible poisoning phenomenon affected the catalyst's activity. The objective of this paper is to present the results of characterization studies on these catalysts. Temperature programmed reduction (TPR) studies suggest that the oxidation–reduction properties of ceria are affected by poisoning. Temperature programmed desorption (TPD) and XPS analysis confirmed the formation of chemisorbed sulfur entities (irreversible poisoning). Based on these findings, a global deactivation mechanism is proposed. Experiments confirmed that the poisoning is reversible and is enhanced at higher temperatures in presence of a reducing environment.

Keywords: Hydrogen; Autothermal reforming; Fuel processing; Sulfur poisoning; Diesel reforming; Catalyst

1. Introduction

Hydrogen generation by reforming hydrocarbon based transportation fuels, such as gasoline, diesel, jet fuel and natural gas has been the focus of research in the past few years. Potential applications include both stationary and mobile fuel cell based power generation units. It is necessary for further research to develop more energy-efficient and compact units for on-board fuel processing [1–4]. Since the focus of our work is fuel reforming, some of the related issues in the reforming processes are addressed.

Catalyst deactivation due to carbon formation is a well-known problem in reforming of hydrocarbon fuels in syngas plants [5,6], particularly for hydrocarbon fuels with two or more carbon atoms in the main chain. Heavier hydrocarbons in the jet fuels and diesel fuels can form carbon deposits even at relatively lower temperatures of 450 °C due to fuel pyrolysis [7]. Fuels with higher aromatic concentration (e.g. diesel) will have a higher tendency of carbon formation.

Hydrocarbon feeds contain sulfur at different concentrations and it is the main force for deactivation of pre-reforming and reforming catalysts [8]. For fuel cell applications, ultra-clean fuels are needed [9], and thus most of the recent discussions in literature on desulfurization of conventional refinery streams to make clean fuels [8] also apply to the fuels for fuel cells. While, coking can be controlled with excess steam and/or oxygen injection, the high sulfur levels in these fuels will require sulfur removal upstream of the reformer [8], if conventional reforming catalysts are employed.

Part I of this paper presented the results of the degradation processes over a 1% Pt/ceria catalyst. This catalyst exhibited good stability for the autothermal reforming (ATR)

* Corresponding author. Present address: Department of Chemical and Biological Engineering, Washington State University, Pullman, WA-99164, USA. Tel.: +1 303 949 1629; fax: +1 509 335 4806.
E-mail addresses: cheek004@bama.ua.edu (P.K. Cheekatamarla), alane@coe.eng.ua.edu (A.M. Lane).

0378-7753/$ – see front matter © 2005 Elsevier B.V. All rights reserved.
doi:10.1016/j.jpowsour.2005.04.011

of synthetic diesel fuel but was severely poisoned by S containing fuel, JP8. Individual effects of some of the sulfur surrogates, such as SO_2 and H_2S, were also discussed. A reversible–irreversible adsorption of sulfur species was observed during the activity/poisoning studies [10].

It is important to study the impact of sulfur and coke contamination on the performance of ATR catalysts. In this study, we correlated the effect of carbon and sulfur and the nature and location of the deposits with a variety of characterization methods (BET, TPR, TPD, XPS, XRD and TGA, etc.). With the aid of these techniques, a global deactivation mechanism is proposed and a concept to effectively counteract catalyst degradation by sulfur poisoning is evaluated.

2. Experimental

ATR catalysts that were used in the activity and poisoning studies discussed in part I were characterized to understand the reaction and/or mechanism/behavior. A description of each of these techniques is given below.

2.1. BET and CO chemisorption measurements

BET surface area of the catalysts was analyzed by nitrogen adsorption–desorption technique. CO chemisorption at −80 °C was utilized to measure the dispersion of these catalysts using the pulse technique; this method is know to avoid to some extent the spillover phenomenon which affects accuracy of the data [11].

2.2. Temperature programmed reduction (TPR) experiments

Temperature programmed reduction was performed in a U-tube quartz reactor using a ChemBET 3000 apparatus manufactured by Quantachrome, provided with thermal conductivity detector (TCD). Pellets (∼0.4 gm) or fine powder (∼0.25 gm) was used. To remove any water and CO_2 adsorbed on the surface, the catalysts were preheated to 250 °C for 2 h followed by purging and cooling in helium. Then a reducing gas mixture consisting of 5% H_2 in helium was passed through the catalyst and the temperature was ramped from 25 to 800 °C at a heating rate of 20 °C min^{-1}.

2.3. Temperature programmed desorption (TPD) experiments

TPD of catalysts was carried out in the ChemBET apparatus described above. In all the TPD experiments, the catalysts were preheated to 250 °C in helium for 2 h to remove residual H_2O and CO_2. After cooling down to room temperature in helium, the catalysts were fed with corresponding gases to study the reactivity. TPD data were acquired in helium at room temperature with a heating rate of 20–600 °C min^{-1}. The flow rate of the gas was typically 70 cm^3 min^{-1}.

2.4. NH_3-TPD experiments

Ammonia TPD studies were also carried out on the ChemBET 3000 instrument. In a typical experiment, ∼4 g of catalyst was taken in a U-shaped quartz tube. Prior to TPD studies, the catalyst was pre-treated by passing high purity helium (40 cm^3 min^{-1}) at 250 °C for 2 h. The catalyst was then saturated by passing ∼50 cm^3 min^{-1} of high purity anhydrous ammonia at 25 °C, and subsequently flushed at room temperature for 2 h to remove the physisorbed ammonia. TPD analysis was carried out from ambient temperature to 600 °C at a heating rate of 20 °C min^{-1}. The ammonia concentration in the effluent stream was monitored with the thermal conductivity detector.

2.5. XPS studies

XPS data were obtained using a Kratos Axis 165 with an Al anode as the X-ray source. These studies were performed on fresh and spent catalysts to identify the changes in surface properties after subjecting the catalysts to activity/stability tests.

2.6. Thermo-gravimetric analysis (TGA)

For gravimetric measurements, a Perkin-Elmer thermogravimetric balance was used. The catalysts were activated under helium atmosphere and the temperature was increased from 25 to 400 °C until a plateau was obtained for the weight.

2.7. X-ray diffraction (XRD)

Powder X-ray diffraction patterns were collected in air on a Philips Powder Diffractometer using Cu Kα radiation with a nickel filter.

3. Results and discussion

3.1. BET surface area and XPS studies

Surface area data of the catalysts used in the activity studies [10] is presented in Table 1. The fresh catalyst had a surface area of 68 m^2 g^{-1}, which decreased significantly down to 33 m^2 g^{-1} when used for ATR of synthetic diesel fuel for 56 h. However, surface area of the catalysts that were used in presence of sulfur [10] was even lower (<15 m^2 g^{-1}),

Table 1
Surface area of the fresh and spent Pt/ceria catalysts used for the autothermal reforming of synthetic diesel and JP8 fuel

Catalyst	Surface area (m^2 g^{-1})
Fresh catalyst	67.7
Spent (synthetic diesel ATR)	33.6
Spent (JP8 ATR)	10.2
Spent (SO_2, synthetic diesel ATR)	14.6

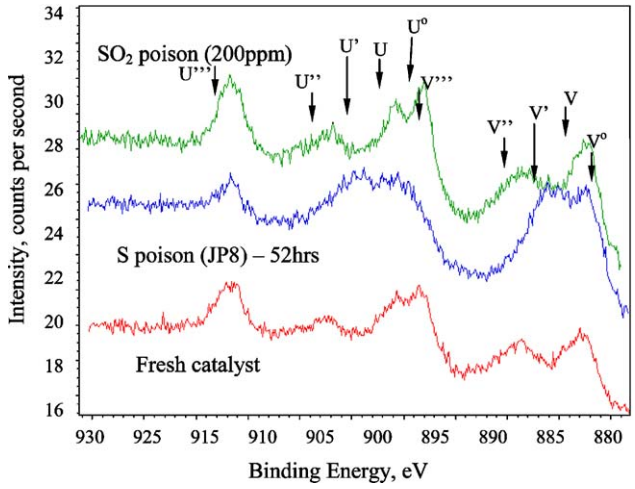

Fig. 1. XPS characterization, Ce 3d spectra of fresh and S-poisoned catalysts.

possibly due to coking in addition to sintering at these operating conditions. Deposition of carbon species was evidenced in the C1s XPS spectra of all the spent samples (not shown). In addition, the presence of sulfur was also noticed on the catalysts utilized in the sulfur poisoning studies (S 2p spectra, 170 eV, not shown). Elemental analysis from XPS studies also showed more carbon on the surface of sulfur-poisoned catalysts compared to that utilized in synthetic diesel ATR. This indeed suggests that the surface area loss is probably due to excess carbon (coking), probably induced by the presence of sulfur-poison.

Fig. 1 shows the Ce 3d spectra of fresh and sulfur-poisoned catalysts. Ce 3d peaks were assigned in accordance with Pfau [12]. Ce 3d envelope for the SO_2 poisoned catalyst is quite similar to that of the fresh catalyst. However, higher V and U intensities in the JP8 poisoned catalyst indicate increased conversion of Ce^{4+} to Ce^{3+} states in this catalyst. The change in oxidation state could be due to the reduction of ceria according to the reaction:

$$6CeO_2 + 3SO_2 \rightarrow Ce_2(SO_4)_3 + 2Ce_2O_3 \quad (1)$$

Fig. 2 shows the Pt 4f XPS spectrum of the fresh and spent catalysts. A positive shift in the Pt $4f_{7/2}$ peak is clearly

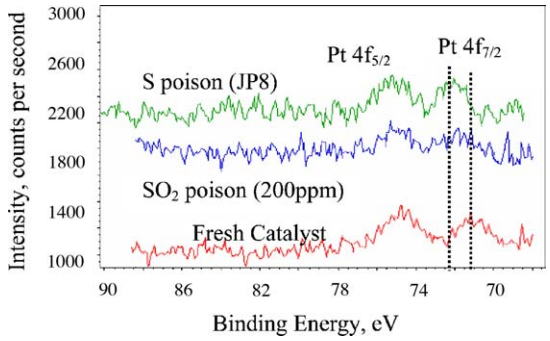

Fig. 2. XPS characterization, Pt 4f spectra of fresh and S-poisoned catalysts.

Table 2
CO-chemisorption data of fresh and spent catalyst; percentage of metal dispersion on the fresh and S-poisoned catalysts

Catalyst	Dispersion (%)
Fresh catalyst	51
Spent (synthetic diesel ATR)	41
Spent (JP8 ATR)	35

evident in the spent catalysts. The shape of the peak in the S-poisoned catalysts was similar, although a difference in the intensity and the peak position can be noticed, with the JP8-poisoned catalyst showing higher signal. The excess metallic Pt intensity in the sulfur-poisoned catalysts may correspond to the formation of surface PtS [13].

Initial evaluation from the XPS studies clearly shows the deposition of carbon and sulfur on the catalyst's surface. It is important to identify these compounds and their location on the catalyst and ways to regenerate the poisoned catalyst by reversing the poisoning mechanism. Further characterization studies were, hence, carried out on these catalysts as discussed in the following sections.

3.2. XRD and CO-chemisorption analysis

An estimation of the X-ray diffraction patterns (not shown) of the fresh and spent catalysts suggests no sintering of the metal under the conditions tested. No evidence of Pt metallic peaks was observed in any of the catalysts tested, and it may be concluded that the average crystallite size of metal for all the catalysts was smaller than 20 nm [14].

Table 2 shows the percentage of metal dispersion of these catalysts. Metal dispersion of the spent catalysts was relatively smaller compared to the fresh catalyst. Since no sintering phenomenon was observed over the tested catalysts, the dispersion loss may be associated with the surface coverage by C and S.

3.3. Temperature programmed reduction studies

H_2-TPR is a convenient way to investigate the reduction/oxygen-storage properties of CeO_2. It gives information on the steps involved in reduction processes and is very sensitive to changes in textural, morphological and structural properties of the oxide [15]. Thus, TPR of ceria was used to characterize the fresh and spent ATR catalysts and associated effects (spillover, metal/support interaction). TPR of ceria is well studied [15] and it typically shows two peaks, one at 500 °C due to the reduction of the most easily reducible surface-capping oxygen of ceria followed by a second one at 900 °C due to the removal of bulk oxygen. Also, the presence of noble metals is known to strongly modify these features due to hydrogen activation by the metal, and consequent migration to the support (spillover) favoring reduction of the ceria surface at lower temperature [16].

Temperature programmed reduction profiles of the fresh and spent catalysts are shown in Fig. 3A–D. For all the cat-

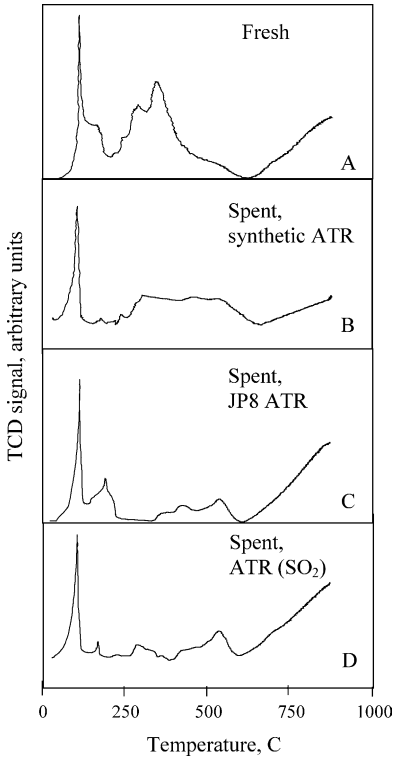

Fig. 3. Temperature programmed reduction profiles of fresh and used catalysts, 5% H_2/N_2 at a temperature ramp of 20 °C min^{-1}.

alysts, the reduction profiles are similar, although there are some differences in both intensity and peak position. Three primary features are associated with the catalyst: a peak in the range 100–125 °C due to the reduction of surface metal oxide; a broad peak in the range 200–600 °C and another one above 600 °C are due to the reduction of bulk ceria support, in agreement with the literature [15]. The peak intensities are smaller in case of spent catalysts suggesting the loss of active sites on the surface. The area of the low-temperature peak (200–600 °C) follows the order: fresh (Fig. 3A) > synthetic diesel ATR (Fig. 3B) > SO_2 poisoned catalyst (Fig. 3D) > S-poisoned (from JP8) catalyst (Fig. 3C). This data exactly reflects the activity behavior of these catalysts for ATR of diesel fuel (activity studies in part I, [10]).

It is known that in the ceria supported catalysts, the reaction mechanism involves oxygen transfer from ceria reacting with molecules, such as CO, CH_4 and other reducing species adsorbed on the metal (Pt) sites. It has been shown that such a mechanism has lower activation energy than the normal oxidation of these molecules on group VIII metals, where reducing species and oxygen adsorb competitively [13,17]. The obvious interpretation of the data from TPR profiles is that sulfur poisoning prevents ceria from transferring oxygen to the metal, so that only the metal function as explained above is observable. The oxidation–reduction properties of ceria probably allow the sulfur-poison to be oxidized which either block the oxygen transfer or affect the redox chemistry of ceria. It seems that the redox property of ceria plays

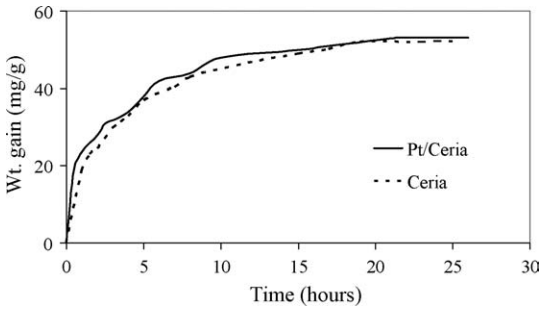

Fig. 4. Variation of catalyst weight with time in presence of SO_2 and an excess of O_2 at 400 °C.

an important role in the autothermal reforming of hydrocarbons, since it is clear from the figure that the oxygen transfer decreases in the same order as the activity of these catalysts [10].

It is also known that most of the hydrogen consumed in the low-temperature region is associated with the removal of the readily available surface oxygen adjacent to the metal through a spillover mechanism [16]. It has been shown [18] that the rate of spillover decreases dramatically in presence of residual species, such as Cl, S, etc. This clearly explains the differences in H_2 uptake as seen in Fig. 3. From the above discussion, it may be concluded that lower hydrogen uptake in the case of low-activity catalysts is possibly due to the hindrance of oxygen mobility in presence of residual sulfur and carbon compounds on the catalytic surface.

3.4. Thermo-gravimetric analysis

ATR experiments in presence of sulfur-laden fuels (JP8, [10]) and sulfur surrogates (SO_2 and H_2S, [10]) showed activity loss with time. Characterization studies performed over the fresh and spent catalysts suggest the deposition of sulfur entities leading to a loss of active sites and the modification of surface properties of ceria. To analyze the deposition behavior of these species during the reaction more accurately, TGA was performed by accumulating sulfate species on the catalyst formed by introducing SO_2 with a large excess of oxygen at 400 °C until reaching a constant weight. For sulfate reduction studies, 20% H_2 in helium was introduced at room temperature followed by heating either at increasing temperature or at 400 °C.

Fig. 4 shows the increase in weight of the two samples, fresh Pt/ceria and ceria support, at 400 °C in presence of oxygen after introduction of SO_2. The mass increase corresponds to total adsorption and oxidation of SO_2 on both the catalysts possibly forming sulfate species on the surface. The two plots are very similar and suggest that the support poisons easily.

The curves of the mass loss due to the reduction of sulfated support and catalyst are illustrated in Fig. 5. It is obvious from the plot that Pt makes the sulfate reduction easier: 3 h to obtain a constant weight for the Pt/ceria catalyst, while 12 h are necessary using the same conditions for the ceria support.

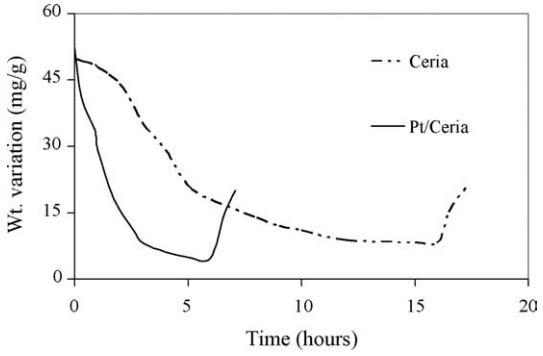

Fig. 5. Variation in the weight of sulfated catalysts (SO_2 and O_2 at 400 °C) with time during reduction and re-oxidation steps by hydrogen and oxygen, respectively.

It also shows the re-oxidation of the reduced catalysts. Re-oxidation by oxygen addition at 400 °C in the thermo-balance leads to a weight gain again possibly due to the formation of sulfur entities from the unreduced species.

Due to the oxidative properties of ceria, SO_2 oxidation occurs even without oxygen and at a relatively low-temperature (∼100 °C) [19]. Literature shows that sulfate reduction under hydrogen flow leads to H_2S formation [20], but the amount of hydrogen introduced under these conditions may not reduce the entire sulfate formed on the catalyst. Some residue sulfur, certainly as cerium sulfide/oxysulfide or as PtS on the catalyst could be the reason for the weight gain during the re-oxidation step. This may possibly explain the difference between reversible and irreversible adsorption of sulfur species as observed in part I [10]. It is possible that after the source of sulfur is removed, the hydrocarbon feed and reducing environment at high temperature removes some of the sulfur entities resulting in a partial revival of the activity leaving behind some of the permanently adsorbed sulfate species. This may be one of the reasons why the original activity was hard to restore.

3.5. Temperature programmed desorption study

Chemisorption and reactivity of SO_2 on fresh and spent catalysts have been studied by temperature programmed desorption. It is already clear from the TPR profiles that the poison affects the ability of ceria to donate oxygen for the reaction of reducing species, leading to a significant decrease in the catalytic activity. TPD study was aimed at understanding the mechanism involved in the formation and decomposition with temperature of various compounds (sulfates or sulfites) on the catalytic surface.

In all the TPD experiments, the catalysts were preheated to 250 °C in helium for 1 h to remove residual H_2O and CO_2. After cooling down to room temperature in helium, the catalysts were covered with: (1) SO_2 at room temperature for 1 h, for SO_2 desorption studies shown in Fig. 6B; (2) O_2 at room temperature for 1 h followed by flushing in He, and then SO_2 at room temperature for 1 h, for SO_2 reactivity with oxygen pre-covered catalyst shown in Fig. 6C; (3) SO_2 at room temperature for 1 h followed by flushing in He, and then CO at room temperature for 1 h, for CO reactivity with SO_2 pre-covered catalyst shown in Fig. 6D.

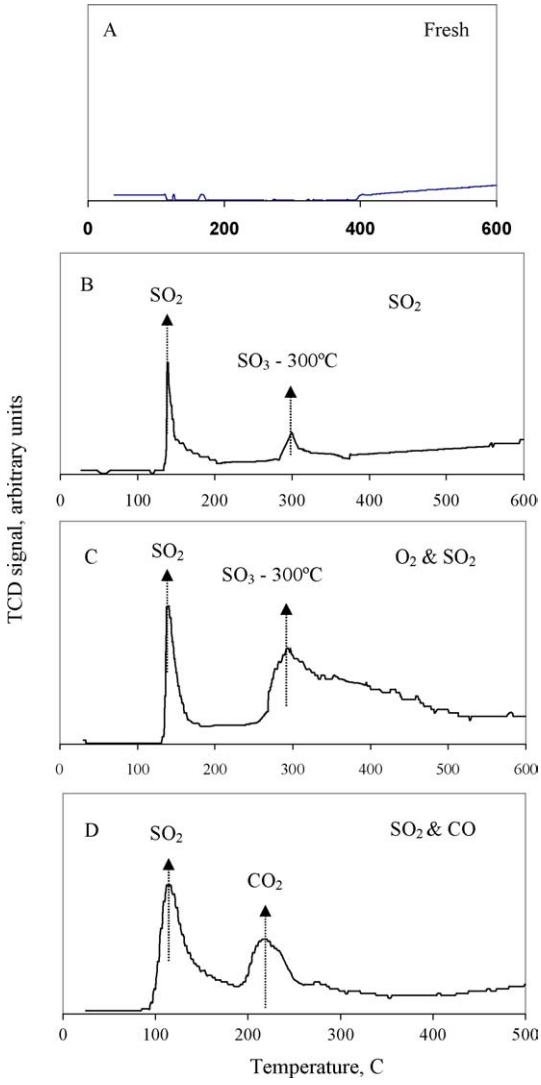

Fig. 6. Temperature programmed desorption profiles of fresh and spent catalysts: (A) TPD in helium; (B) SO_2 desorption in He; (C) SO_2 adsorption on O_2 pre-covered sample and (D) SO_2 adsorption on CO pre-covered sample.

TPD data were acquired in helium at room temperature with a heating rate of 20–600 °C min^{-1}. The flow rate of all the gases was typically 70 cm^3 min^{-1}. Fig. 6A shows desorption profile over the fresh catalyst, this can be treated as the base line for the rest of the experiments. No desorption peaks were observed over the temperature range tested. Two SO_2 desorption features are observed in the TPD spectra obtained after SO_2 chemisorption on clean Pt catalyst. The presence of pre-adsorbed oxygen leads to the appearance of a new feature, which can be attributed to that of SO_3 desorption [21].

Fig. 6B and C shows TPD spectra obtained after saturation doses of SO_2 at room temperature on clean and oxygen pre-covered catalysts. SO_2 adsorption at room temperature yields

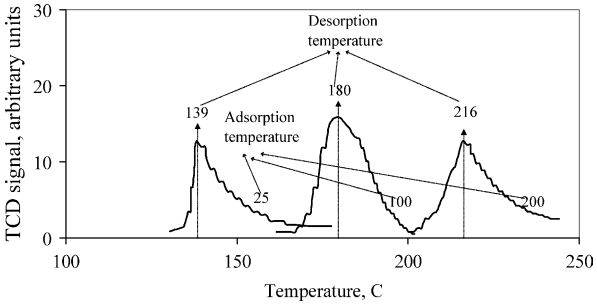

Fig. 7. SO_2 desorption from a fresh Pt/ceria catalyst at different adsorption temperatures.

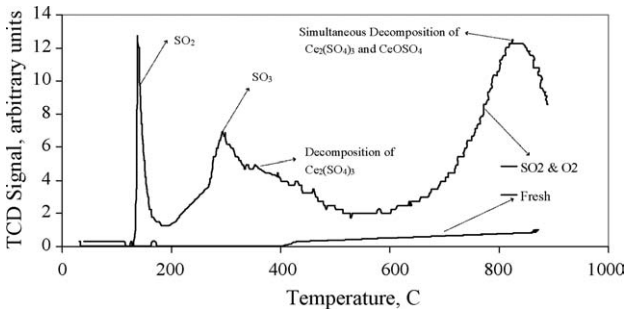

Fig. 8. TPD of fresh catalyst and SO_2 and O_2, pre-covered catalyst.

a desorption feature at ~120–140 °C followed by a small desorption peak in case of the clean catalyst and a broad peak in case of the oxygen pre-covered catalyst, both at 300 °C. We assign the first peak at to SO_2 desorption and the 300 °C peak to SO_3 desorption [21]. The huge difference in size of the SO_3 desorption peak can be explained by the difference in the amount of oxygen coverage over the two catalysts.

The adsorbed SO_2 molecule can also react with CO, H_2 or CH_4 following the dissociative chemisorption of SO_2 [22], and therefore we investigated the reactivity of SO_2 towards CO. The result of this experiment is shown in Fig. 6D and it is relevant to understanding the SO_2 induced inhibition of the autothermal reforming reactions. Experiments were performed at room temperature by dosing with CO on SO_2 pre-covered catalyst, which yielded two desorption features, the first one at ~140 °C due to SO_2 desorption followed by a broad peak at ~220 °C due to CO_2 desorption [22].

SO_2 adsorption at higher temperatures gives further insight in to the nature of the adsorption and desorption behavior of the surface species. In order to study this behavior, SO_2 was adsorbed at temperatures varying from 25 to 200 °C. The results of this experiment are shown in Fig. 7. It can be noticed that the desorption temperature is directly proportional to the adsorption temperature. Due to the high operating temperatures inside the autothermal reformer, and hence higher SO_2 adsorption temperature, desorption can occur at higher temperatures resulting in the formation of sulfate species that are difficult to desorb. This may be verified by comparing the desorption profiles of the used catalyst with that of a fresh catalyst at a higher temperature range.

Decomposition of different commercial sulfates was reported as a function of temperature and it is known that certain cerium sulfites and sulfates, such as $Ce_2(SO_4)_3$ and $CeOSO_4$, decompose at temperatures above 700 °C [23]. Fig. 8 corresponds to temperature programmed desorption profiles of fresh, pre-adsorbed (with SO_2 and O_2) catalyst, both of which were pre-treated to remove residual water and CO_2. There was no sign of desorption peaks over the fresh catalyst. However, four distinctive peaks were observed on the pre-adsorbed catalyst. The lower temperature peaks are due to dioxide and trioxide desorption as discussed above. The peak at 350 °C can be attributed to $Ce_2(SO_4)_3$ [24].

The peak at 820 °C corresponds to the simultaneous decomposition/desorption of $Ce_2(SO_4)_3$ and $CeOSO_4$ in agreement with the literature [23]. Distinction between different sulfur compounds of cerium is well studied [23,25], based on these observations, it can be concluded that the less stable surface species, such as $S_2O_7^{2-}$ decompose at $T < 450$ °C, however, other species such as $CeOSO_4$ and $Ce_2(SO_4)_3$ are still present at 800 °C [26]. Analysis of the above experiments clearly shows that some of the sulfur species associated with the support can be decomposed at 450 °C and most of it can be removed at higher temperatures. Also, from the TGA results it was concluded that in a reducing atmosphere most of the poison species could be removed. If this is true, the deactivated catalyst should retain most of its initial activity when subjected to a reducing atmosphere at temperatures above 800 °C.

We followed upon this observation from the TPD and TGA analysis that the S-poison ($Ce_2(SO_4)_3$) from deactivated catalysts decompose in a reducing environment at higher temperatures ($T > 800$ °C). An experiment was conducted to reactivate the S-poisoned (JP8) spent catalyst. A fresh Pt catalyst was utilized in the ATR of JP8 fuel until a significant decrease in the activity was observed followed by a regeneration treatment at 800 °C under a constant flow of 20% hydrogen for 30 min. This catalyst was then tested for its autothermal reforming activity under the same conditions as reported in part I [10] and the results are shown in Fig. 9. It can be noticed that the Pt catalyst was completely

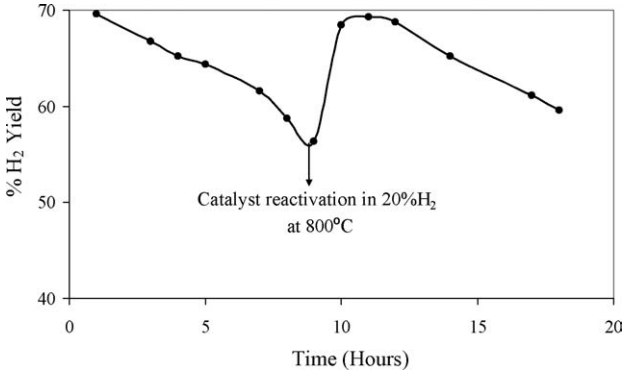

Fig. 9. ATR activity of Pt/ceria catalyst after treating the poisoned catalyst at 800 °C in 20% H_2 in helium for 30 min.

Table 3
Acidity measurements on fresh and spent Pt/ceria catalysts during the NH_3-TPD analysis

Catalyst	Intermediate acidity	Strong acidity
Fresh catalyst	Yes	Yes
Spent (synthetic diesel ATR)	Yes	Yes
Spent (JP8 ATR)	Yes (low)	None

reactivated, hydrogen yield improved to a value of 69% compared to 56% from the poisoned catalyst. However, the hydrogen yield decreased later during the experiment again because of the poisoning effect. This experiment indeed confirms the fact that the poisoning is reversible and is enhanced at higher temperatures in presence of a reducing environment.

3.6. NH_3-temperature programmed desorption study

It is well-known that the acid–base properties of the catalysts play a role in chemical reactions (activity, selectivity and stability). Temperature programmed desorption of ammonia is a well-known method for the determination of acidic strength of catalysts. TPD curves suggest a reasonable picture of the distribution of the acid sites on the catalyst surface. In the present study, the acidity measurements have been carried out by ammonia TPD method.

In a typical experiment, ~400 mg of catalyst was utilized. Prior to TPD studies, the catalyst was pre-treated by passing pure helium at 250 °C for 2 h followed by saturation with high purity anhydrous ammonia at 25 °C, and subsequently flushed at room temperature for 2 h to remove the physisorbed ammonia. TPD analysis was carried out from ambient temperature to 600 °C at a heating rate of 20 °C min^{-1}. The ammonia concentration in the effluent stream was monitored with the thermal conductivity detector.

Three catalysts viz. fresh Pt/ceria, spent (synthetic ATR) and spent (JP8 ATR) were tested to find their respective acid strengths. They were chosen to find out correlation between change in activity and acidic strength of the catalyst. The variation in ATR catalytic activity of these catalysts is reported in part I [10]. It is well-known that a low/high NH_3 desorption temperature corresponds to weak/strong acid sites [27]; accordingly, two classes of acid sites are currently identified: weak-intermediate (100–350 °C) and strong (>600 °C) [28,29]. These features are based on the reaction temperature range observed for the ATR of synthetic diesel fuel. Intermediate acidity corresponds to the reactor temperature (start-up, 400 °C) and strong acidity to the maximum conversion zone (most active reactions, ~800 °C). Since the tested catalysts had different surface areas, only a qualitative analysis of these observations is presented here and a quantitative estimation of the number of acid sites cannot be done.

Fig. 10 presents the ammonia TPD profiles for the catalysts tested and Table 3 represents corresponding acidity characteristic over each of the catalysts. The reference Pt/ceria catalyst (fresh) exhibits a broad distribution of acidic strengths with desorption peaks corresponding to intermediate acid sites

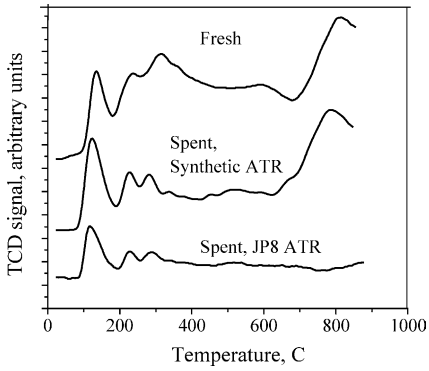

Fig. 10. Results of temperature programmed desorption (TPD) of NH_3 over fresh and spent ATR catalysts.

in the temperature range 100–350 °C and strong acid sites at temperatures above 600 °C. The other two used catalysts exhibit similar distributions of acid strengths for the intermediate acidities. However, for the catalyst used in JP8 ATR, the desorption peak associated with strong acidity totally disappeared suggesting a drop in the total acidity of the catalyst w.r.t reference. Also, it is known that acid-type oxide carriers provide further possibilities for stabilization of small metal particles by their accommodation as metal-proton adducts. This may be one of the reasons for the activity drop over this catalyst, possibly caused by instable metal particles over the less-acidic carrier/support. The catalyst used for synthetic diesel ATR exhibited acid strength distributions close to the reference in line with the activity data presented in part I [10].

These results show that the S-poison from the JP8 fuel induces very important changes in the amount of acidity and in the acid strengths distribution possibly due to the formation of new species as evidenced in the TPD and XPS results. As a result, we assume that strong acidities play a major role in diesel autothermal reforming because they were significantly modified by the presence of poisonous species.

4. Poisoning mechanism

XPS analysis confirmed an increased conversion of Ce^{4+} to Ce^{3+} states in the spent catalyst, which may partially be due to formation of sulfites according to reaction (1). It is generally assumed that the formation of poisonous species on the reducible oxides changes the surface, chemical and structural characteristics [30]. This fits well with the results observed over the fresh and used catalysts in the temperature programmed reduction profiles and surface area measurements, where a decrease in the mobility of oxygen (from the support) was observed.

In light of the above results related to the adsorption, diffusion and desorption of sulfur-poison on the catalyst, we propose a mechanism as shown in Fig. 11 that is responsible for the loss in partial activity of the ceria supported Pt catalyst. The characterization data from the XPS, TPR, TPD and BET analysis supports this hypothesis.

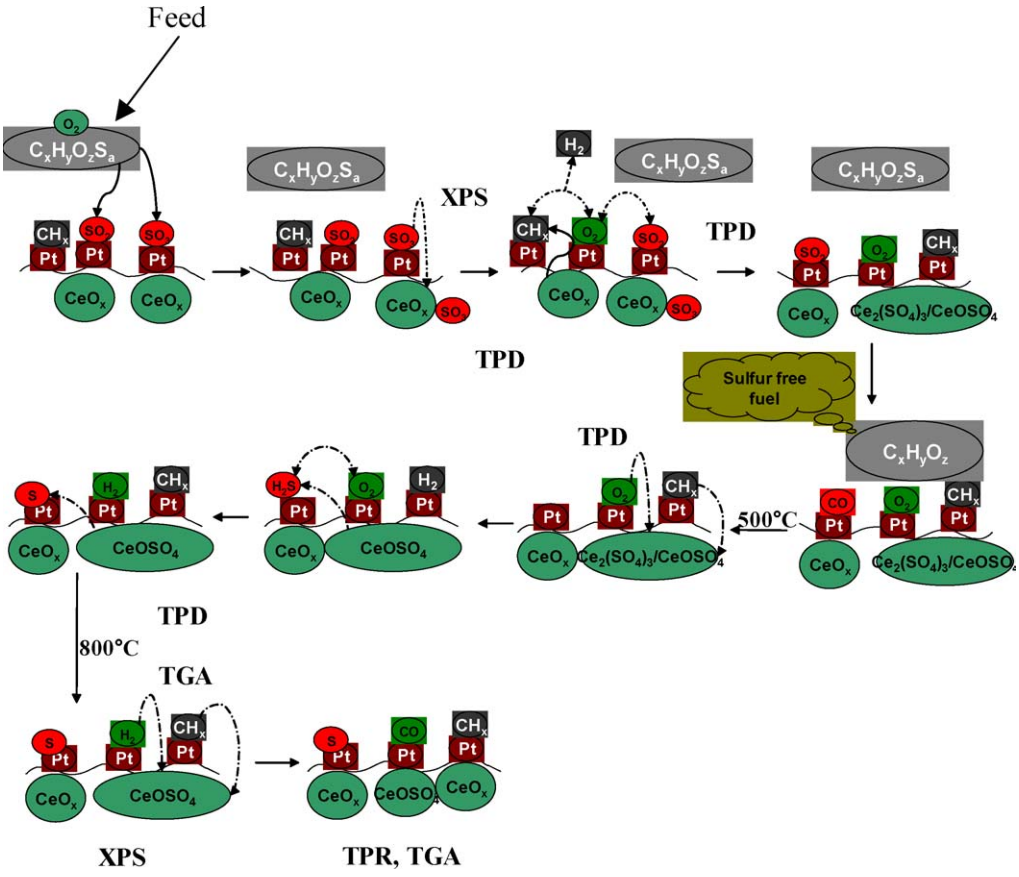

Fig. 11. Reaction/poisoning mechanism (adsorption, diffusion, desorption) deduced from experimental results and surface characterization analysis.

The Pt with sulfating ceria support adsorbs SO_2 and SO_3 formed from sulfur contained in the diesel fuel (evident from Pt 4f, S 2p XPS spectra). During the reactions, the support interacts with SO_3, protecting the active sites on the surface. The adsorption of SO_3 by the support (resulting in the formation of cerium sulfates and sulfites as observed in the TPD studies) decreases the rate of the reaction. When the poisonous source is removed from the gas stream, SO_3 desorbs from the support, spills onto the active metal sites and continues the suppression of diesel reforming activity.

Combined with the TPD results, TGA analysis allow us to deduce the following reaction pathway: SO_2 adsorbed on the ceria surface species close to Pt would be easily oxidized to SO_3 (as observed in the TPD, TGA results) leading to the formation of sulfate species. These surface species then migrate into the ceria bulk in the presence of SO_3 excess. Pt, increasing the SO_3 formation favors the sulfate diffusion in the ceria support (TGA results). A higher surface area leads to a larger amount of adsorbed SO_3 on ceria catalysts [31,32]. TPD analysis showed that some of the bulk like species disappear first and are not present at lower temperatures ($T < 450\,^{\circ}C$) on ceria, while some surface sulfate species are still adsorbed at 800 °C.

Table 4 shows the free energy values for the formation and dissociation of certain compounds proposed in the mechanism. Even at temperatures of 400 °C, sulfates and sulfites of ceria are easier to form. However, in a reducing atmosphere, the sulfites are easier to dissociate than the sulfates (free energy values), in line with the observations made during TPD studies.

Finally, from TGA and TPD analysis it is clear that the entire sulfate formed on the support was not removed even in the presence of reducing environment (reaction gases, H_2 and CH_4) resulting in a permanent loss of some activity due to the irreversible adsorption/chemisorption of sulfur entities that impede the mobility of oxygen (from the support) to the active sites (as observed in the TPR studies).

Finally, by combining the findings stated above, the following overall deactivation mechanism is proposed:

$$Pt + SO_2 \rightarrow Pt\text{–}SO_2 \quad (2)$$

Table 4
Free energy values for different compounds (formation, dissociation) proposed in the mechanism

Reactants	Products	ΔG (kcal mol^{-1}, 400 °C)	ΔG (kcal mol^{-1}, 800 °C)
SO_2, O_2	SO_3	−16.94	–
SO_3, CeO_2	$CeOSO_4$	−18.43	–
SO_3, CeO_2	$Ce_2(SO_4)_3$	−72.82	–
$CeOSO_4$, H_2	CeO_2, H_2S	182.5	103.09
$Ce_2(SO_4)_3$, H_2	CeO_2, H_2S	268.9	187.96

$$2Pt\text{–}SO_2 + O_2 \rightarrow 2Pt\text{–}SO_3 \quad (3)$$

$$4Pt\text{–}SO_3 + 2CeO_2 + \tfrac{5}{2}O_2 \rightarrow Ce_2(SO_4)_3 + CeOSO_4 + 4PtO \quad (4)$$

(reaction rate high at higher temperatures)

$$CeOSO_4 + H_2 \rightarrow CeO_2 + SO_2 + H_2O \; (T \sim 400\,^{\circ}C) \quad (5)$$

$$Ce_2(SO_4)_3 + 2H_2 \rightarrow 2CeO_2 + 3SO_2 + 2H_2O \quad (6)$$

($T > 750\,^{\circ}C$, sulfur free environment)

5. Conclusions

Based on the results from the characterization studies on fresh and spent catalysts used in autothermal reforming of diesel fuel presented in part I, a global deactivation mechanism responsible for activity loss is proposed. The deposition and diffusion of certain poisoning compounds like carbon and sulfates/sulfites of ceria was found to deactivate the catalyst. Results from TPD and TGA suggest a regeneration technique, according to which, the poisoning is reversible in a hydrogen atmosphere and is enhanced at high temperatures.

Acknowledgements

The material in this paper was based upon work supported by the U.S. Army National Automotive Center, Ballard Power Systems, and the Center for Advanced Vehicle Technologies at The University of Alabama.

References

[1] B.D. McNutt, L.R. Johnson, Competing against entrenched technology: implications for U.S. government policies and fuel cell development, in: Presented at the Pre-Symposium Workshop of the Sixth Grove Fuel Cell Symposium, London, UK, September 1999.
[2] R.A.J. Dams, P.R. Hayter, S.C. Moore, The processing of alcohols, hydrocarbons and ethers to produce hydrogen for PEMFC for transportation applications, SAE-paper 97109.
[3] A.P. Meyer, C.R. Schroll, R. Lesieur, Development and evaluation of multi-fuel fuel cell power plant for transport applications, SAE-paper 2000-01-0008, SP-1505.
[4] S. Wieland, F. Baumann, K.A. Startz, Proceedings of the Fuel Cell Seminar on New Catalysts for Autothermal Reforming of Gasoline and Water-Gas Shift Reaction, Portland Oregon, 2000.
[5] J.R. Nielsen, Carbon limits in steam reforming, Paper presented at Fouling Science and Technology, NATO ASI Series, Series E, 1988, p. 405.
[6] Y. Sone, et al., J. Power Source 86 (2000) 334.
[7] C. Song, S. Eser, P.G. Hatcher, Energy Fuels 7 (1993) 234.
[8] J.R. Nielsen, T.S. Christensen, I. Dybkjaer, Stud. Surf. Sci. Catal. 113 (1998) 81.
[9] C. Song, Catalysis and chemistry for deep desulfurization of gasoline and diesel fuels. An overview, in: Fifth International Conference on Refinery Processing, AIChE 2002 Spring National Meeting Proceedings, New Orleans, 2002, p. 3.
[10] P.K. Cheekatamarla, A.M. Lane, J. Power Source, in press.
[11] B. Andersson, D. Duprez, Appl. Catal. B: Environ. 22 (1999) 215.
[12] L.G. Pfau, K.D. Schierbaum, Surf. Sci. 321 (1994) 71.
[13] H.C. Yao, Y.F.Y. Yao, J. Catal. 86 (1984) 254.
[14] C.E. Mixan, J.B. Lambert, J. Org. Chem. 38 (1973) 350.
[15] C.de. Leitenburg, A. Trovarelli, J. Kaspar, J. Catal. 166 (1997) 98.
[16] D. Teschner, et al., Solid State Ionics 141 (2001) 709.
[17] E.S. Putna, T. Bunluesin, Catal. Today 50 (1999) 343.
[18] M. Waqif, A.M. Saad, M. Benstiel, J. Chem. Soc. Faraday Trans. 88 (1992) 2931.
[19] O. Saur, J.C. Lavalley, G. Blanchard, Appl. Catal. B: Environ. 13 (1997) 265.
[20] J.A.M. Kuipers, W.P.M. Swaaij, Catal. Today 66 (2001) 427.
[21] C. Hardacre, C.J. Baddeley, J. Ludecke, Surf. Sci. 372 (1997) 279.
[22] E. Shustorovich, et al., J. Mol. Catal. A: Chem. 119 (1997) 367.
[23] C.J. Chuang, et al., Appl. Catal. B: Environ. 12 (1997) 309.
[24] A.F. Diwell, C. Hallett, J. R. Taylor, Catalysts for hydrogen generation from HC fuels, Society of Automotive Engineers, Paper 872163, 1987.
[25] M. Waqif, et al., Appl. Catal. B: Environ. 11 (1997) 103.
[26] G. Blanchard, et al., Appl. Catal. B: Environ. 15 (1998) 345.
[27] S.J. Teichner, Appl. Catal. 62 (1990) 1.
[28] C. Apesteguia, T. Garretto, A. Borgna, J. Catal. 106 (1987) 73.
[29] H.C. Nelson, R.J. Lussier, M.E. Still, Appl. Catal. 7 (1983) 113.
[30] P. Berteau, B. Delmon, Catal. Today 5 (1989) 121.
[31] D.S. Maciver, H.H. Tobin, R.T. Barth, J. Catal. 2 (1963) 485.
[32] U.A. Sedran, N.S. Figoli, Appl. Catal. 19 (1985) 317.